

# Avoiding cracks and inhomogeneities in billets processed by ECAP

Paulo R. Cetlin · Maria Teresa P. Aguilár ·  
Roberto B. Figueiredo · Terence G. Langdon

Received: 23 January 2010 / Accepted: 3 March 2010 / Published online: 18 March 2010  
© Springer Science+Business Media, LLC 2010

**Abstract** Although equal-channel angular pressing (ECAP) is now an established technique for producing bulk ultra-fine-grained metallic materials, processing difficulties may arise because of the occurrence of cracking or inhomogeneities. This problem is examined with reference to experimental data for aluminum and magnesium alloys and a Pb–Sb alloy. It is shown that effective procedures are available for avoiding the development of inhomogeneities and the cracking of billets during ECAP: these procedures include introducing a pre-deformation of the as-cast material prior to ECAP, decreasing the strain produced in each ECAP pass by using dies with angles higher than 90°, and controlling the rotation of the billets between sequential passes.

## Introduction

From the point of view of the end user, ultrafine-grained (UFG) metallic materials display interesting mechanical properties. Among the various available procedures for the production of UFG materials, equal-channel angular pressing (ECAP) [1] is the most established method for the production of bulk billets, which usually have circular or rectangular cross-sections.

Processing by ECAP has been applied to a wide range of materials, such as pure aluminum, copper, magnesium, titanium, iron, and their alloys. In practice, the billets obtained from ECAP are well suited for the production of small parts such as dental implants [2] and they are especially attractive where a small grain size is imperative in order to circumvent undesirable grain size effects in the material flow and/or in the final shapes of the processed parts.

The use of ECAP billets in any commercial applications demands a controlled and predictable grain size, a constant cross-section, an absence of cracking, and an overall homogeneity of the properties, which is related to the homogeneity of plastic deformation in the material. For many products, a general isotropy of the mechanical properties may be desirable whereas for other applications, as in micro-sheet metal drawing, a controlled anisotropy of the material deformation may be desirable.

It is now well established that ECAP processing may introduce significant damage, in the form of shear bands, cracking, and segmentation, into the processed material. Numerous procedures have been adopted in attempts to avoid the development of cracking and deformation inhomogeneities during the processing operation. These procedures include (i) using ECAP dies having angles larger than 90° [3–5], (ii) conducting the processing at a low

---

P. R. Cetlin (✉) · R. B. Figueiredo  
Department of Metallurgical and Materials Engineering,  
School of Engineering, Federal University of Minas Gerais,  
Belo Horizonte, MG 30160-030, Brazil  
e-mail: pcetlin@demet.ufmg.br

M. T. P. Aguilár  
Department of Materials Engineering and Construction,  
School of Engineering, Federal University of Minas Gerais,  
Belo Horizonte, MG 30160-030, Brazil

R. B. Figueiredo · T. G. Langdon  
Materials Research Group, School of Engineering Sciences,  
University of Southampton, Southampton SO17 1BJ, UK

T. G. Langdon  
Departments of Aerospace & Mechanical Engineering  
and Materials Science, University of Southern California,  
Los Angeles, CA 90089-1453, USA

speed [6–9], (iii) increasing the processing temperature [7, 9], (iv) the use of preliminary deformation step [10, 11], and (iv) incorporating a back-pressure into the pressing operation [12–14].

Earlier study focused on the use of finite-element modeling (FEM) to understand plastic flow and damage accumulation during ECAP [5, 15–17]. This research was undertaken to provide experimental evidence for the occurrence of cracks and shear localization in ECAP and to use mechanical testing to evaluate the significance and the sources of any softening that may occur during the processing operation.

## Experimental materials and procedures

Several different materials were incorporated into this investigation in order to provide a comprehensive understanding of the problems of cracking and inhomogeneities.

First, an Al–1.3 wt% Fe–0.6 wt% Mg–0.1 wt% Si alloy was received in the form of extruded rods with  $15.6 \times 15.6 \text{ mm}^2$  square cross-sections, and these rods were annealed at 513 K for 90 min. Processing by ECAP was conducted at a pressing speed of  $\sim 0.3 \text{ mm s}^{-1}$  using a split die with an angle of  $90^\circ$  between the two channels and without any external curvature. Further details concerning the ECAP processing of the aluminum alloy were given earlier [16].

Second, a Pb–4.5 wt% Sb alloy was cast in the laboratory from commercial purity Pb and Sb. The material was cast into ingots with  $16 \times 16 \text{ mm}^2$  square cross-sections and processed by ECAP in the same die used for the processing of the aluminum alloy but with a higher pressing speed of  $\sim 5 \text{ mm s}^{-1}$ .

Third, two magnesium alloys, AZ31 (Mg–3 wt% Al–1 wt% Zn) and ZK60 (Mg–5.5 wt% Zn–0.5 wt% Zr), were received as extruded rods with 10 mm diameter cross-sections: henceforth, this is designated the extruded condition for both alloys. These rods were cut into billets and processed by ECAP using solid dies with angles of either  $90^\circ$  or  $110^\circ$  between the two channels, with an external arc of curvature of  $20^\circ$ , and with the processing conducted at temperatures from 473 to 513 K. Further details of the ECAP processing of the magnesium alloys were given earlier [5, 18].

The structure of the aluminum alloy was evaluated by optical microscopy under polarized light. Samples from the longitudinal plane were extracted before and after ECAP, and these samples were ground and polished to a mirror-like finish. Electrolytic etching was carried out using Baker's reagent [19].

The structure of the lead alloy was evaluated on the longitudinal planes of the billets before and after ECAP.

The samples were ground and polished to a mirror-like finish and etched in a solution of acetic acid and  $\text{H}_2\text{O}_2$ . Some samples were overetched in order to facilitate the observation of the distribution of the Sb-rich areas. These samples were observed using scanning electron microscopy (SEM). Further details on the ECAP processing of the lead alloy and the structural evolution were given earlier [20]. It should be noted that the deformation direction is horizontal in all images of the structures of both the lead and the aluminum alloys.

Compression tests were carried out on the aluminum alloy after processing by two passes of ECAP and on the lead alloy before and after ECAP. The compression specimens were cylindrical with a diameter of 6 mm and a height of 9 mm, and they were cut parallel to the axial direction of the billets. Tensile specimens were machined from the ZK60 magnesium alloy in the as-received condition, in an annealed condition, and after one pass of ECAP. These specimens had a gauge length of 4 mm and a cross-section of  $2 \times 3 \text{ mm}^2$ . It is important to note that compression tests are attractive in determining the flow behavior of a material because the results are more accurate at large strains and the tests provide information on the occurrence of any flow softening.

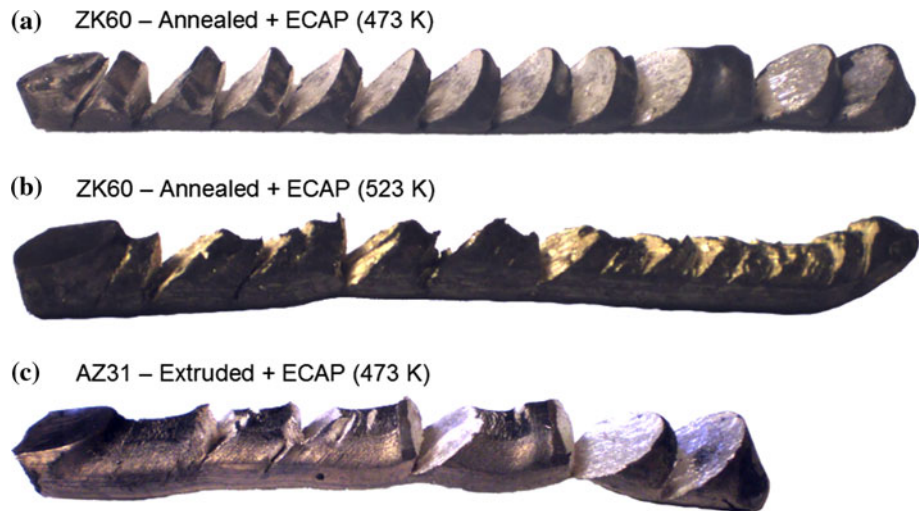
## Experimental results

The development of damage and heterogeneous flow during ECAP

### *Magnesium alloys*

Experimental cracking of the billets was observed when processing the magnesium AZ31 alloy in the extruded condition and the ZK60 alloy after annealing at 673 K for 4 h. The billets cracked during ECAP when using a solid die with  $90^\circ$  between the channels, pressing temperatures in the range 473–523 K and punch speeds of  $\sim 10$ – $20 \text{ mm s}^{-1}$ . Figure 1 shows the appearance of representative billets after pressing under different conditions. It is observed in Fig. 1a that the annealed ZK60 exhibits large cracks throughout a large fraction of the cross-section when processing at 473 K. For this sample, the billet shows the occurrence of regular segmentation in which the billet has become divided into relatively uniform and discrete segments linked together by very small remaining portions of the cross-section along the bottom surface. It is apparent in Fig. 1b that the alloy also exhibits cracks when pressing at a higher temperature of 523 K but it is apparent that, unlike at 473 K, some of these cracks do not propagate through the entire cross-section of the billet. The extruded

**Fig. 1** Evidence of segmentation in billets of magnesium alloys: ZK60 (a) and (b) in an annealed condition and AZ31 (c) in an extruded condition after processing for one pass of ECAP



AZ31 alloy shown in Fig. 1c exhibits cracking when processed at 473 K, and some cracks propagate almost through the total cross-section of the billet, whereas most of the cracks are reasonably localized along the upper surface. It is also apparent from inspection of the billets in Fig. 1 that there is a significant reduction in the heights of the cross-sections of the billets after processing by ECAP where this is indicative of the occurrence of flow softening [17].

*Lead alloy*

The as-cast lead alloy also cracked when processed at room temperature using the split die with a punch speed of  $\sim 5 \text{ mm s}^{-1}$ . Figure 2 shows the appearance of a typical billet after pressing for one pass. It was observed in this

alloy that the cracks are initiated at the upper surface and extend toward the center of the billet.

*Aluminum alloy*

The aluminum alloy was successfully processed at room temperature through two passes of ECAP following route  $B_c$ , where the billet is rotated by  $90^\circ$  in the same sense between consecutive passes [21]. However, shear bands were observed after three passes using route  $B_c$  as shown in Fig. 3, which is a low magnification image of the longitudinal plane of the billet. The wavy aspect of the structure visible in Fig. 3 is due to the unstable flow during ECAP. Some superficial cracking was also observed on the top surface of the billet as reported earlier [16], but these cracks failed to propagate through the cross-section.

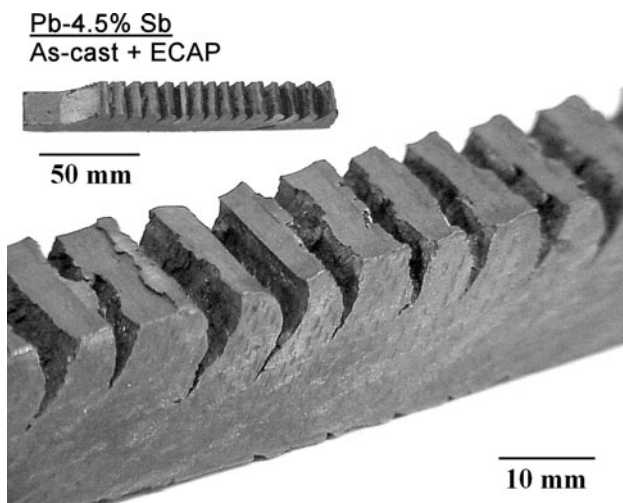


**Fig. 2** Cracking and segmentation in a lead alloy processed by ECAP for one pass from the as-cast condition: the cracks initiate at the top surface and propagate to the mid-section

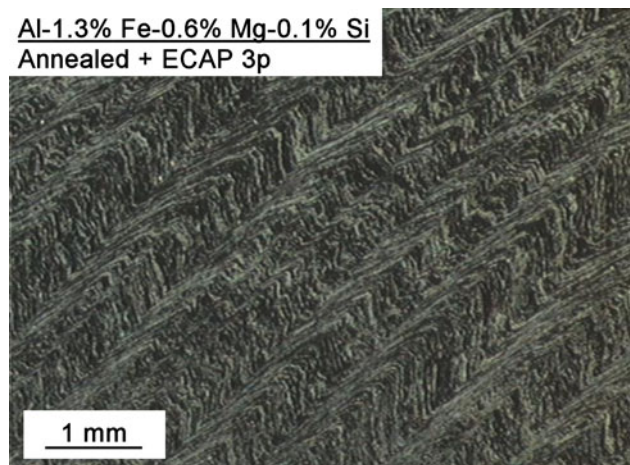


**Fig. 3** Longitudinal section of the aluminum alloy after processing for three passes using route  $B_c$

## Characterization of the structure

### Lead alloy

Two phases are observed in the Pb–4.5% Sb alloy: the lead-rich matrix and the eutectic, which consists of lamellae of an antimony-rich phase. The chemical etching used in the samples preferentially attacks the lead-rich matrix, and therefore, the eutectic phase may be readily observed. Figure 4 shows the structure of the lead alloy revealed by SEM (a) in the as-cast condition and (b) after ECAP: the sample after ECAP was cut from the lower volume of the billet where the cracks failed to propagate. It is observed that the eutectic phase has no preferential orientation in the as-cast material, but it attains a preferential orientation in some layers after ECAP. These layers are aligned at  $\sim 45^\circ$  to the billet axis, which lies horizontally in Fig. 4b. For ease of inspection, broken dashed lines are drawn in Fig. 4b to distinguish the layers having preferential alignment of the eutectic from the layers where the eutectic exhibits no significant alignment. The apparent pattern in the orientation of the eutectic phase after ECAP shows that the billet has undergone unstable flow such that some layers have been subjected to larger amounts of shear.

Figure 5 shows the grain structure observed in the lead alloy after ECAP through one pass. The grain boundaries were revealed by performing rapid chemical etching and the structure was observed in an area where the eutectic exhibited preferential alignment so that this area underwent significant plastic deformation during ECAP. It is apparent from Fig. 5 that the grains are not elongated, thereby confirming that recrystallization has taken place in this alloy during or after the ECAP processing.

### Aluminum alloy

The structure of the aluminum alloy before and after ECAP, as observed using polarized light microscopy, is

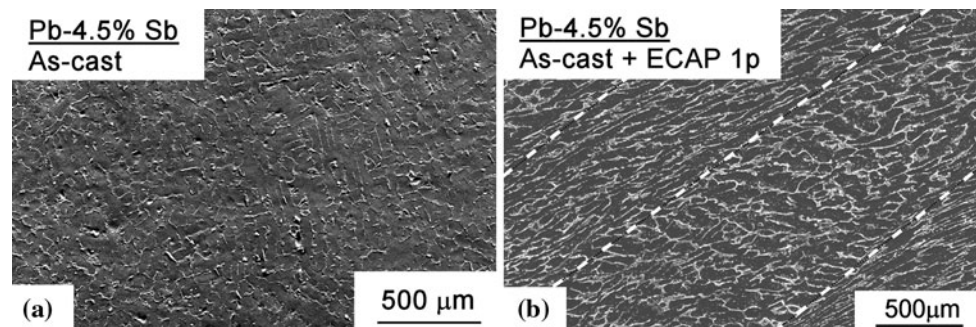


**Fig. 4** Structure of the lead alloy in SEM **a** before and **b** after ECAP where the bright areas are rich in antimony: the *broken dashed lines* distinguish different amounts of deformation in (b)

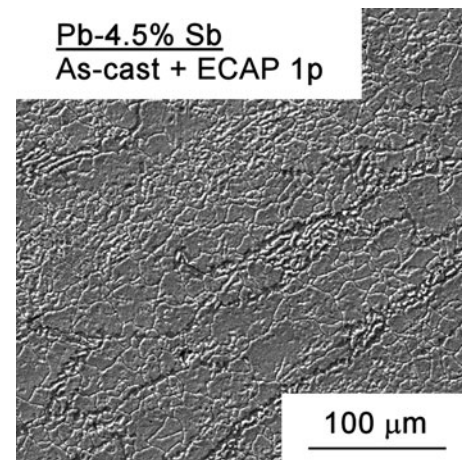


**Fig. 5** Grain structure on the longitudinal plane of the lead alloy after processing by ECAP for one pass

shown in Fig. 6. Equiaxed grains are observed in the annealed condition before ECAP processing in Fig. 6a, where the dark areas are iron-rich intermetallics that became aligned to the billet axis during the extrusion process before the annealing. Figure 6b shows the structure after one pass of ECAP where the grains are elongated and aligned due to the plastic deformation. Careful observations showed that the structure was similar throughout the billet except only at the front edge and at the tail, thereby indicating that stable flow takes place during ECAP. A similar structure, representative of stable flow, was also visible after two passes. However, shear bands were observed in several areas of the billet after the third pass of ECAP as shown in Fig. 6c. The microstructure in Fig. 6c was recorded on the longitudinal plane with the billet axis lying horizontal, and it demonstrates the presence of layers with different levels of shear strain. This observation shows that there is a transition from stable flow in the second pass to unstable flow during the third pass of ECAP in the aluminum alloy.

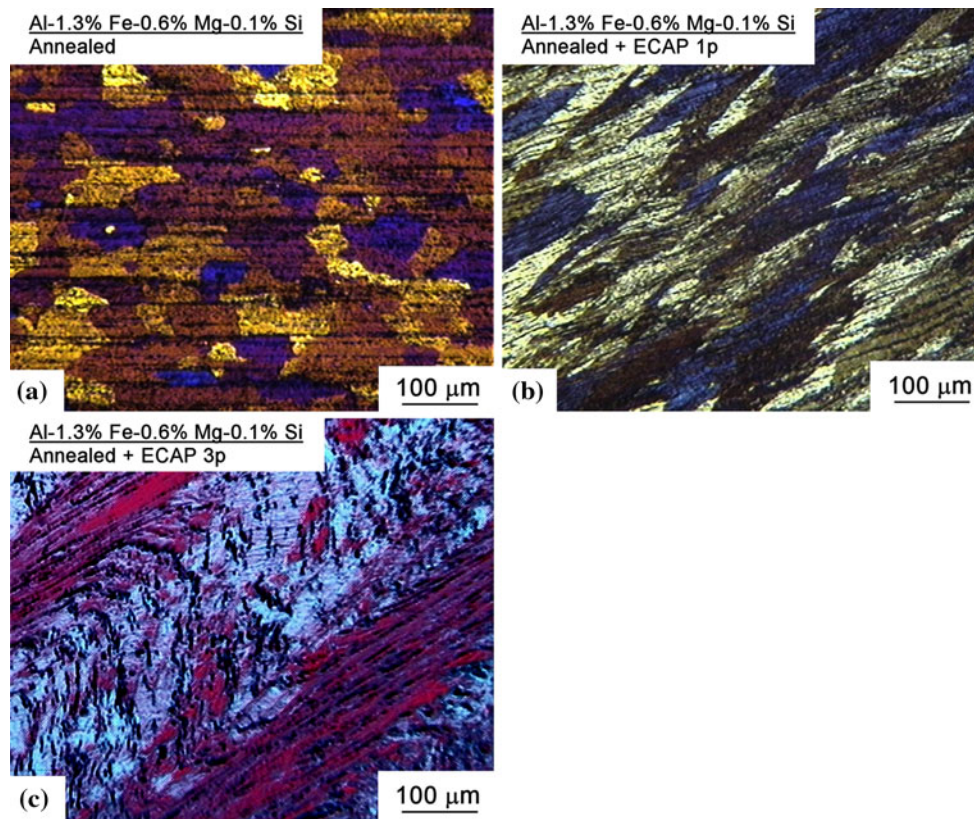


**Fig. 6** Structure of the aluminum alloy observed under polarized light microscopy **a** in the annealed condition and after **b** one pass and **c** three passes of ECAP

Flow behavior

*Magnesium alloy*

Figure 7 gives the stress–strain curves obtained by tensile testing of the ZK60 alloy in three different conditions: after annealing the extruded condition for 4 h at 673 K to give a grain size of  $\sim 180 \mu\text{m}$ , in the initial extruded condition

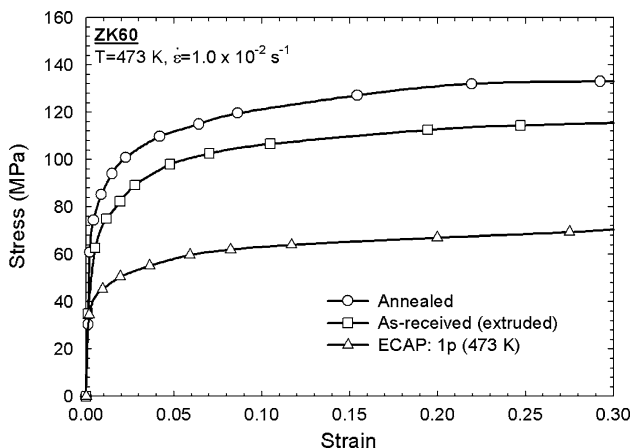


**Fig. 7** Stress–strain curves at 473 K for the ZK60 magnesium alloy tested under different conditions

where the grain size was  $\sim 2.9 \mu\text{m}$ , and after ECAP of the extruded condition for one pass to give a grain size of  $\sim 1.0 \mu\text{m}$ . The tests were carried out at 473 K, which corresponds also to the ECAP processing temperature, using an initial strain rate of  $1.0 \times 10^{-2} \text{ s}^{-1}$ . Inspection shows that the annealed material exhibits the highest flow stress, the extruded material has an intermediate flow stress, and the material processed by ECAP has the lowest flow stress. As already documented in an earlier report [18], the annealed material has a coarse grain structure, the extruded material has an intermediate grain structure, and the material processed by ECAP has the finest grain structure. Thus, the curves in Fig. 7 show that lower flow stresses are observed when the grain structure is refined within the temperature and strain rate range corresponding to the ECAP processing conditions. Although finer grain structures are usually associated with higher strength, the opposite trend is observed when testing at high temperatures as finer structures facilitate diffusion processes.

*Lead alloy*

Compression tests were conducted on the lead alloy at room temperature (298 K), and Fig. 8 shows the stress–

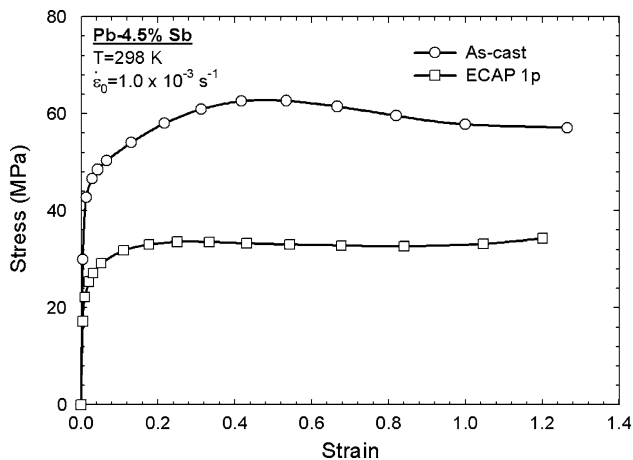


**Fig. 8** Stress–strain curves for the lead alloy before and after ECAP through one pass [20]

strain curves for the material both in the as-cast condition before ECAP and after processing by ECAP for one pass. The flow curves for both conditions exhibit an initial strain hardening up to a peak stress, a slight flow softening, and then deformation under a quasi-steady-state condition. These curves suggest the presence of dynamic recrystallization for both conditions. It is apparent also that the as-cast material has a larger flow stress than its counterpart processed by ECAP. This shows that the flow stress is dependent upon the structure as the as-cast material had a relatively coarse grain structure of  $\sim 250 \mu\text{m}$ , whereas the material processed by ECAP had a much finer grain size of  $\sim 12 \mu\text{m}$  [20]. It is important to note also that lead has a low-melting temperature, and deformation at room temperature will be assisted by diffusion mechanisms, which explains the lower flow stress in the sample with the finer structure.

#### Aluminum alloy

Figure 9 shows a stress–strain curve for the aluminum alloy processed by ECAP for two passes at room temperature and then tested in compression at the same temperature using a high strain rate of  $1.0 \text{ s}^{-1}$ . It is observed that this material exhibits a rapid hardening up to a strain of  $\sim 0.03$ , a softening up to  $\sim 0.23$ , and then a flow stress that does not vary significantly at even larger strains. In fact, a very minor increase in flow stress was observed at the highest strains but this was attributed to friction effects during compression testing. This result shows that the strain hardening capability of the material is essentially exhausted after two passes of ECAP.

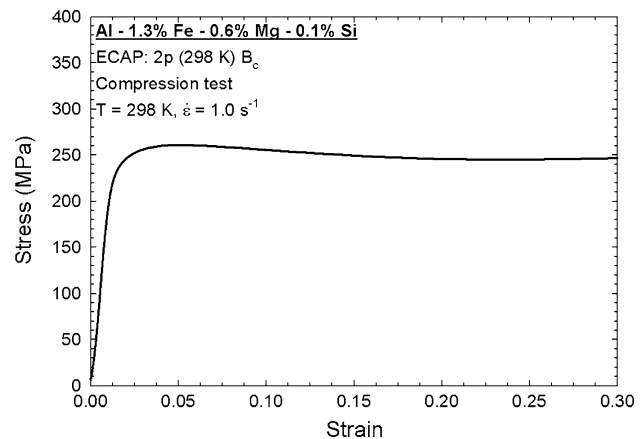


**Fig. 9** Stress–strain curve for the aluminum alloy processed through two passes of ECAP

#### Discussion

The deformation inhomogeneity in billets produced by ECAP

A critical problem associated with deformation inhomogeneity in ECAP processing is the presence of deformation bands in the billets which are a consequence of cyclic variations in the deformation level. Figures 4b and 6c show examples of such bands in the lead and aluminum alloys, respectively. The Pb–4.5% Sb alloy is an especially convenient model material for an experimental analysis of plastic flow due to its low flow stress and the presence of a eutectoid phase, which permits a clear visualization of the flow patterns.

It is instructive to note that the formation of such bands was analyzed quite early in the history of ECAP using slip line field theory [6] and later it was confirmed using FEM simulations [15]. An analytical description was presented recently [22]. It is now clear that flow softening is an important requirement for the occurrence of unstable flow. In practice, the material in the deformation zone develops a level of flow stress, which is below that of the incoming unprocessed material and, as a consequence, the unprocessed material is no longer deformed as it penetrates the shearing zone. This forces a rotation of the material undergoing shear and it moves away from the geometrically defined shearing zone until the stress necessary for further straining in this new position surpasses the stress required to start a new deformation band in the geometrically defined shearing region [15]. The process is cyclic in nature, and it leads to the creation of successive deformation bands in the processed billet as shown experimentally in Fig. 3 for the aluminum alloy.

Strain softening may be caused by (i) adiabatic heating, (ii) dynamic recrystallization (DRX), (iii) softening associated with a breakdown of the initially as-cast structure, (iv) changes in the strain path or by a combination of these various factors. It is important to note, however, that the sensitivity of the flow stress of the material to strain rate changes may serve to alleviate or even fully suppress the occurrence of these deformation bands. These various possibilities are now examined.

#### Softening by adiabatic heating

Adiabatic heating of the material and its attendant softening is unavoidable and it is directly related to the pressing speed, the deformation level imposed in a single pass and the characteristics of the material including the flow stress. A simple solution to the problem is to reduce the pressing speed and thereby to incorporate a reduced heating of the material due to heat transfer to the die walls. Other possibilities are either to increase the angle within the ECAP die or to increase the pressing temperature. For the former route, the strain level and thus the associated energy is decreased, and for the latter route, the energy is also decreased because there is a reduction in the flow stress.

Early reports described the occurrence of flow localization and cracking in copper [6], aluminum [8], titanium [10, 23], and steel [23] processed by ECAP at a high punch speed but with essentially steady flow when the pressing was performed at lower speeds. These observations show that adiabatic heating plays a significant role in promoting failure during ECAP. The present results demonstrate the occurrence of flow localization in an aluminum alloy after only three passes of ECAP, and in this condition, the strain hardening capability of the material is virtually exhausted so that the higher flow stress leads to more heat generation during the pressing operation. In practice, however, the pressing speed used in the present experiments was only  $\sim 0.3 \text{ mm s}^{-1}$ , and this is significantly lower than the speed where adiabatic heating is observed in different materials [6, 8, 23]. This low pressing speed allows a rapid dissipation of heat and minimizes the softening effect associated with adiabatic heating.

#### Softening by changes in the material strain path

It is well known that changes in the strain path of the material may lead to transients in the flow curve, which include changes in the yield stress during reloading, additional hardening and material softening, characterized by a negative slope in the stress–strain curve. For ECAP, such strain path changes are most directly associated with the various processing routes that can be utilized when undertaking successive paths through the die. Any accurate

description of the material behavior in ECAP depends upon a determination of the strain path and the undertaking of tests with changes in the orientation of loading. For example, it is established that deformation occurs on the same slip plane but in an opposite direction in successive passes using route C [24] where the billet is rotated by  $180^\circ$  between successive passes [21]. In order to accurately predict the flow behavior of a material during sequential passes of ECAP through route C, it is important to change the sense of deformation during the test. A recent study determined the stress–strain curves to be utilized for ECAP by route C through reversed torsion curves [25]. These curves displayed hardening transients but no softening and, as a consequence, no deformation bands were observed in the FEM simulation of the second pass of ECAP following route C [25].

By contrast, the usual processing routes of A without any billet rotation and  $B_c$  with billet rotations by  $90^\circ$  in the same sense [21] are associated with dislocation phenomena that are far more complex than the simple slip reversals expected for route C. As a result, it is reasonable to anticipate these changes in strain path will be more susceptible to transients and to flow softening. Furthermore, this conclusion is consistent with experimental data for Cu [26–29] and Al [29, 30] where samples were tested in compression along different directions after processing by ECAP. The stress–strain curve for the pure aluminum processed by two passes of ECAP and compressed along the billet axis [29] was similar to that observed in the present experiments and shown in Fig. 9. The softening observed in pure aluminum was successfully modeled by considering transients in the strain path changes [29]. Thus, the softening observed in the aluminum alloy in the present experiments is attributed to strain path changes where these changes are expected to lead to cross-slip when pressing using route  $B_c$ . It follows, therefore, that a change in the processing route from  $B_c$  to C should eliminate the occurrence of cross-slip because shear then occurs in a reverse direction on the same plane during sequential ECAP passes. Further experiments are now needed to check this conclusion.

#### Softening by dynamic recrystallization (DRX)

The stress–strain curves of the Pb–4.5% Sb alloy show this material undergoes DRX at room temperature. Generally, the softening caused by DRX depends on the temperature, strain rate, and grain size [31]. Many reports have documented the occurrence of DRX in magnesium alloys deformed at temperatures close to  $\sim 500 \text{ K}$  where the ECAP processing is usually conducted [32–35]. Thus, both the lead alloy processed at room temperature and the magnesium alloys processed at  $473 \text{ K}$  are expected to

exhibit softening due to DRX when processing by ECAP. Simulations by FEM were used in an earlier report to show that the softening due to DRX in magnesium alloys may lead to unstable flow during ECAP if the strain rate sensitivity of the material is limited [17].

It was reported that a magnesium alloy with an initial finer grain structure displayed reduced peak strains and low softening caused by DRX [34]. Such fine grains can be obtained by thermo-mechanical processing of the material before ECAP and, consistent with this concept, it has been observed that such pre-processing is useful as a first preliminary step in order to avoid the cracking of Mg during ECAP [11, 36]. The elimination of DRX softening during ECAP may also be achieved by using dies with higher angles leading to lower strains in the shearing zone [5]. Thus, if these strains are below the strain for the onset of DRX, no softening will be observed.

The present results on the lead alloy show the occurrence of DRX in compression tests. However, the softening observed in the stress–strain curve is very limited and stable flow is expected due to the strain rate sensitivity of the material. An earlier report showed this alloy may be successfully processed from the as-cast condition for up to eight passes of ECAP at a pressing speed of  $\sim 0.3 \text{ mm s}^{-1}$  without any cracking and with no evidence of flow localization [20]. The present experiments were conducted using a similar material and processing conditions except only that the pressing speed was increased to  $\sim 5 \text{ mm s}^{-1}$ . This suggests that the pressing speed plays a key role in the occurrence of plastic instabilities and cracking. Similar results were also reported for a magnesium AZ31 alloy [9], which exhibited cracks when the ECAP was conducted at high speeds at 473 K but with perfect uncracked billets when the pressing speed was significantly reduced.

#### Softening by the breakup of the initial as-cast structure

Figure 8 displays the stress–strain curves for the Pb–4.5% Sb alloy in an as-cast condition and after processing by ECAP for 1 pass. It is apparent that the material is significantly softened by ECAP, but it is difficult to identify whether this softening is associated only with the mechanical breakup of the as-cast structure during processing by ECAP or whether it relates to static softening following the deformation since the alloy undergoes static recrystallization at room temperature. Figure 5 shows that the grains in the matrix of the alloy are equiaxed and appear fully recrystallized after ECAP. An earlier report demonstrated there was a significant decrease in the hardness of the lead alloy after a single pass of ECAP [20]. Thus, since this hardness remains unchanged after further processing, it appears that the softening is due to the breakup of the initial as-cast structure.

In order to check the role of any break-up of the as-cast structure of the lead alloy, some billets were subjected to deformation using a small rolling facility prior to processing by ECAP. The billets were rolled in two passes with a 1-mm reduction in thickness in each pass to a final cross-section of  $15 \times 15 \text{ mm}^2$  and with the billets rotated by  $90^\circ$  between passes in order to retain the square cross-section. After this deformation, the billets were stored for 24 h for complete recovery and then processed by ECAP using the same pressing speed of  $\sim 5 \text{ mm s}^{-1}$  used for the billets exhibiting cracking. No cracks were observed in the billets subjected to rolling before ECAP, thereby confirming that the cracks observed in the lead alloy are due to a softening of the as-cast structure. It should be noted that this is in agreement with the reports of enhanced formability in ECAP of different materials when applying a prior step of deformation [10, 11, 36].

#### The effect of the strain rate sensitivity

The flow stress of a metal is sensitive to the externally imposed strain rate. It is known that tensile deformation is more stable in materials displaying a high strain rate sensitivity because in this deformation mode the increase in strain rate in incipient necks leads to an increase in the flow stress in these regions such that necking is then interrupted and transferred to some other region. This delay in necking thereby produces an increase in the tensile elongation.

The situation in ECAP has similarities to flow in tension in the sense that the strain rate in the shearing region is much higher, as in the tensile region of necking, than in the material outside this region. This means that the increase in flow stress of the material caused by the increase in strain rate can offset the softening effects already discussed and thus eliminate the formation of deformation bands in the material. An earlier report [5] showed that an increase in the strain rate sensitivity of materials processed by ECAP leads to a broadening of the deformation zone within the shearing region in ECAP.

The tendency for unstable flow in ECAP may be quantified by the parameter  $\alpha$ , which is defined as [23, 37]

$$\alpha = \frac{\gamma'}{m}, \quad (1)$$

where  $m$  is the strain rate sensitivity of the material and the term  $\gamma'$  is associated with the flow softening through the expression:

$$\gamma' = -\frac{\partial \ln \sigma}{\partial \ln \dot{\epsilon}}, \quad (2)$$

where  $\sigma$  is the flow stress and  $\dot{\epsilon}$  is the true strain. Plastic instability is believed to take place in ECAP if the



parameter  $\alpha$  is larger than  $\sim 5$  [37]. A direct consequence is that an increase in the strain rate sensitivity may prevent the occurrence of plastic instability. The prediction of the occurrence of plastic instability for values of  $\alpha$  larger than  $\sim 5$  is also supported by FEM simulations [17].

The cracking of billets during processing by ECAP

Ductile cracking is associated with the simultaneous occurrence of deformation and predominantly tensile stress states. This is, for example, the basis of the normalized Cockroft–Latham ductile fracture criterion, which is described mathematically by the relationship [38, 39]:

$$C_N = \int \frac{\sigma_T}{\sigma} d\varepsilon, \quad (3)$$

where  $\sigma_T$  is the maximum principal stress and  $C_N$  is a critical level of damage that leads to cracking of the material. It is also widely known that the imposition of external hydrostatic pressures can delay or even totally eliminate the occurrence of ductile fracture, as demonstrated in the classic early experiments of Bridgman [40].

Cracking may be avoided either by decreasing the amount of strain or by decreasing the level of the tensile stresses during the metal-working process. The former is achieved by increasing the die angle in ECAP [5] and the latter is achieved by imposing a back-pressure in the exit channel [13]. However, cracking is usually associated with the development of intermittent deformation bands in the material, as clearly indicated in Fig. 10 for the aluminum alloy where the cracking occurs at the deformation bands in the third pass of ECAP.

The intensity of deformation banding and the maximum deformation within the bands is also of significant importance in the ductile cracking of materials processed by ECAP. This was the situation, for example, in experiments on commercial purity titanium where billets exhibiting a large distance between the deformation bands failed by flow localization, whereas there was no failure in billets having closely spaced deformation bands [7].

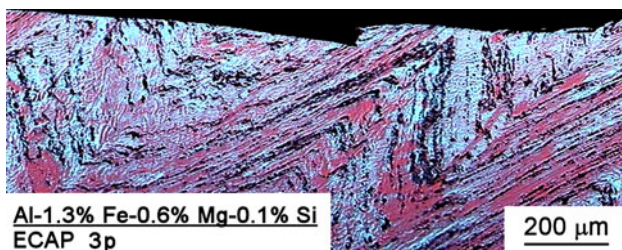


**Fig. 10** Structure at the top of the billet of the aluminum alloy after processing through three passes of ECAP: a crack is visible at the top of the billet near a shear band

## Summary and conclusions

1. Processing by ECAP using dies with an angle of  $90^\circ$  between the channels produces cracking and segmentation in a Pb–4.5% Sb alloy, cracking and segmentation in the AZ31 and ZK60 magnesium alloys, and flow localization in an aluminum alloy.
2. The cracks in the lead and magnesium alloys are due to flow softening arising from a refinement of the initial coarse-grained structure, and the flow localization in the aluminum alloy is due to strain path effects.
3. Flow softening may be avoided during ECAP by undertaking a preliminary processing of the as-cast materials. The use of ECAP processing route C is also favorable to reduce the tendency for flow localization due to the strain path effects.

**Acknowledgements** This study was supported by the National Science Foundation of the United States under Grant No. DMR-0855009. PRC and MTPA are grateful for the financial support of CNPq (Brazilian National Research Council), CAPES (Post-Graduate Commission of the Education Ministry of Brazil), and FAPEMIG (Foundation for the Support of Research in Minas Gerais State).

## References

1. Valiev RZ, Langdon TG (2006) Prog Mater Sci 51:881
2. Valiev RZ, Semenova IP, Latysh VV, Rack H, Lowe TC, Petruzelka J, Dluhos L, Hrusak D, Sochova L (2008) Adv Eng Mater 10:B15
3. Aleksandrov IV, Raab GI, Shestakova LO, Kil'mametov AR, Valiev RZ (2002) Phys Met Metallogr 93:493
4. Furui M, Kitamura H, Anada H, Langdon TG (2007) Acta Mater 55:1083
5. Figueiredo RB, Cetlin PR, Langdon TG (2007) Acta Mater 55:4769
6. Segal VM (1999) Mater Sci Eng A271:322
7. Semiatin SL, DeLo DP (2000) Mater Des 21:311
8. Fagin PN, Brown JO, Brown TM, Jata KV, Semiatin SL (2001) Metall Mater Trans 32A:1869
9. Kang F, Wang JT, Peng Y (2008) Mater Sci Eng A487:68
10. DeLo DP, Semiatin SL (1999) Metall Mater Trans 30A:2473
11. Horita Z, Matsubara K, Makii K, Langdon TG (2002) Scr Mater 47:255
12. Stolyarov VV, Lapovok R, Brodova IG, Thomson PF (2003) Mater Sci Eng A357:159
13. Lapovok RY (2005) J Mater Sci 40:341. doi:10.1007/s10853-005-6088-0
14. Xu C, Xia K, Langdon TG (2009) Mater Sci Eng A527:205
15. Figueiredo RB, Aguilar MTP, Cetlin PR (2006) Mater Sci Eng A430:179
16. Figueiredo RB, Cetlin PR, Langdon TG (2009) Mater Sci Eng A518:124
17. Figueiredo RB, Cetlin PR, Langdon TG (2010) Metall Mater Trans A 41:778
18. Figueiredo RB, Langdon TG (2009) Mater Sci Eng A501:105
19. Slámová M, Ocenáček V, Vander Voort G (2004) Mater Charact 52:165
20. Figueiredo RB, Costa ALM, Andrade MS, Aguilar MTP, Cetlin PR (2006) Mater Res (Revista Ibero-Americano de Materiais Brazil) 9:101

21. Furukawa M, Iwahashi Y, Horita Z, Nemoto M, Langdon TG (1998) *Mater Sci Eng A* 257:328
22. Lapovok R, Tóth LS, Molinari A, Estrin Y (2009) *J Mech Phys Solids* 57:122
23. Semiatin SL, Segal VM, Goforth RE, Frey ND, DeLo DP (1999) *Metall Mater Trans* 30A:1425
24. Furukawa M, Horita Z, Nemoto M, Langdon TG (2001) *J Mater Sci* 36:2835. doi:[10.1023/A:1017932417043](https://doi.org/10.1023/A:1017932417043)
25. Figueiredo RB, Pinheiro IP, Aguilár MTP, Modenesi PJ, Cetlin PR (2006) *J Mater Proc Technol* 180:30
26. Alexander DJ, Beyerlein IJ (2005) *Mater Sci Eng A* 410–411:480
27. Beyerlein IJ, Li S, Alexander DJ (2005) *Mater Sci Eng A* 410–411:201
28. Beyerlein IJ, Tome CN (2007) *Int J Plast* 23:640
29. Beyerlein IJ, Alexander DJ, Tomé CN (2007) *J Mater Sci* 42:1733. doi:[10.1007/s10853-006-0906-x](https://doi.org/10.1007/s10853-006-0906-x)
30. Xu C, Száráz Z, Trojanová S, Lukáč P, Langdon TG (2008) *Mater Sci Eng A* 497:206
31. Humphreys FJ, Hatherly M (1995) *Recrystallization and Related Annealing Phenomena*. Pergamon Press, Oxford
32. Ion SE, Humphreys FJ, White SH (1982) *Acta Metall* 30:1909
33. Galiyev A, Kaibyshev R, Gottstein G (2001) *Acta Mater* 49:1199
34. Beer AG, Barnett MR (2006) *Mater Sci Eng A* 423:292
35. Al-Samman T, Gottstein G (2008) *Mater Sci Eng A* 490:411
36. Matsubara K, Miyahara Y, Horita Z, Langdon TG (2003) *Acta Mater* 51:3073
37. Semiatin SL, Segal VM, Goetz RL, Goforth RE, Hartwig T (1995) *Scr Metall Mater* 33:535
38. Cockcroft MG, Latham DJ (1968) *J Inst Met* 96:33
39. Oh SI, Chen CC, Kobayashi S (1979) *J Eng Ind* 101:36
40. Bridgman PW (1952) *Studies in large plastic flow and fracture*. McGraw-Hill, New York